Technische Universität Graz
Institut für Chemische Verfahrenstechnik und Umwelttechnik

Phase and Interfacial behavior of the ternary system Toluene / Ethanol / Water

Jorge Alonso-Collada Aza

Graz, July 2018

Jorge Alonso-Collada Aza

Phase and Interfacial behavior of the ternary system Toluene / Ethanol / Water

Bachelor Thesis

In fulfilment of the requirements for the degree of

Bachelor of Science

in

Process Engineering

submitted at

Graz University of Technology

Supervisor:

Univ.-Prof. Dr.-Ing. habil. Tim Zeiner

Dipl.-Ing. Roland Nagl, BSc

Institute of Chemical Engineering and Environmental Technology

Graz, July 2018

Deutsche Fassung:

Beschluss der Curricula-Kommission für Bachelor-, Master- und Diplomstudien vom 10.11.2008

Genehmigung des Senates am 1.12.2008

EIDESSTATTLICHE ERKLÄRUNG

Ich erkläre an Eides statt, dass ich die vorliegende Arbeit selbstständig verfasst, andere als die angegebenen Quellen/Hilfsmittel nicht benutzt, und die den benutzten Quellen wörtlich und inhaltlich entnommenen Stellen als solche kenntlich gemacht habe.

Graz, am …… ……

(Unterschrift)

Englische Fassung:

STATUTORY DECLARATION

I declare that I have authored this thesis independently, that I have not used other than the declared sources / resources, and that I have explicitly marked all material which has been quoted either literally or by content from the used sources.

Graz, …… ……

date (signature)

Abstract

Equilibrium data in ternary liquid-liquid systems is necessary for the design of extraction processes. Interfacial tension is an important parameter in mass transfer models, and therefore highly relevant in extraction. Thus, experimental measurements of these parameters are a prerequisite for the development of industrial processes.

This work analyzes the interfacial behavior of the water-ethanol-toluene system by experimentally determining equilibrium tie lines and interfacial tensions at 25 °C. A total of five concentration points was analyzed. Each point was measured three times.

Concentrations at equilibrium were determined using gas chromatography for ethanol and toluene, and a Karl-Fischer titrator for water content.

Interfacial tensions were measured using a spinning drop tensometer. Phase densities and refractive indexes were also measured, all of them at 25 °C.

The obtained equilibrium data was found to be inconsistent with previous literature data. This was probably caused by errors in the experimental method. Interfacial tension measurements were consistent with previous experiments, and it was found to decrease with ethanol content, as was expected.

Contents

1 Introduction

1.1 Liquid-Liquid extraction processes

Liquid-liquid extraction is an operation in which a component of a liquid mixture is separated by putting it in contact with a solvent. This solvent should be immiscible in the mixture, but present high solubility for the desired component. It can be used to separate a valuable component from a mixture, or for purification processes.

It is widely utilized in chemical engineering processes at an industrial level, particularly in cases in which distillation is not viable.

Design of extraction processes requires an understanding of the ternary equilibrium between the extracted component and the two solvents. Equilibrium concentrations determine the effectiveness of the extraction and equipment size, and by extension the viability of a process.

Thus, experimental analysis of the system is necessary [1].

1.2 Motivation: Interfacial tension in LLE

In extraction processes, mass transfer takes place across an interface between the two liquids. The exact nature of this interface is not fully understood today, but interfacial properties play a crucial role in mass transfer and as such determine the effectivity of an extraction.

Models like the density gradient theory (DGT) attempt to predict mass transfer across the interface [2]. Interfacial tension is a vital parameter in these models and can be measured experimentally in a number of ways.

Thus, experimental analysis of the interfacial properties of a variety of systems is vital to refining and validating these models.

2 State of the art

2.1 Liquid/liquid equilibrium (LLE)

The most common phase equilibria in separation processes are the vapour-liquid equilibrium (VLE), the liquid-liquid equilibrium (LLE) and the solid-liquid equilibrium (SLE).

Phase equilibrium occurs when the Gibbs energy minimizes and entropy maximizes, at which point each component in each phase has constant temperature, pressure and chemical potential.

The study of this equilibrium state is of vital importance in the field of chemical engineering, since it heavily impacts mass transfer between phases, and therefore the design of separation processes and equipment.

In the case of LLE, results show that the equilibrium state is very dependent on temperature, but the influence of pressure it usually negligible [1]. The simplest cases dealt with in the industry are ternary systems in which one component is soluble in both immiscible phases.

A commonly used tool for analyzing ternary LLE data are triangular diagrams, in which each extreme of the triangle represents a component. Fig. 2-1 shows a typical ternary diagram for liquid-liquid extraction. The extremes of a tie line represent the concentrations in each phase when they are in equilibrium with each other. The binodal curve is drawn along the extremes of all tie lines and separates the 2-phase region from the single phase one.

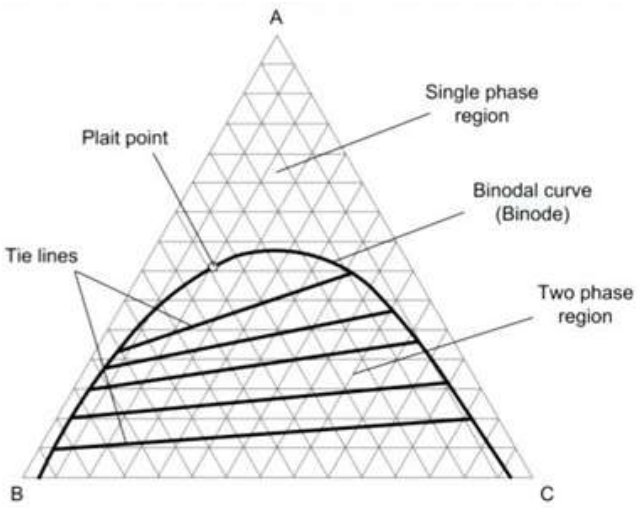

Fig. 2-1: Example diagram for a ternary liquid-liquid extraction system [9]

The tie lines for a certain system and at a certain temperature can be determined experimentally with relative ease. Mixtures of known concentrations within the two phase region are prepared and then allowed to reach equilibrium. Subsequently, the concentrations in each phase are determined analytically (see section 3, *Experimental methods*).

2.1.1 Liquid-liquid extraction

Liquid-liquid extraction is a process for separating components in solution by their distribution between two immiscible liquid phases. One example is liquid-liquid extraction of an impurity from wastewater into an organic solvent.

It is used primarily when distillation is impractical or too costly to use. An important factor in determining the effectivity of distillation for a given mixture is the relative volatility of the components, defined as

$$\alpha = \frac{(y_i/x_i)}{(y_j/x_j)} = K_i/K_j$$

α: the relative volatility of the more volatile component to the less volatile component.

y_i: the vapor–liquid equilibrium concentration of component i in the vapor phase.

x_i: the vapor–liquid equilibrium concentration of component i in the liquid phase

(y/x): Henry's law constant (also called the K value or vapor-liquid distribution ratio) of a component

Extraction may be more practical than distillation when the relative volatility for two components is bellow 1.2. Likewise, liquid-liquid extraction may be more economical than distillation or steam-stripping when the relative volatility of the solute to water is less than 4. It may also be used when one or more of the components are heat sensitive, such as antibiotics, or non-volatile, like mineral salts [2].

Generally, at least three components are involved in an extraction. To make the description of the process simpler, key components are defined. The feed to a liquid – liquid extraction is the solution that contains the components to be separated. The solvent is the liquid added to the process to extract a valuable component from the feed. The solvent can be a pure component, but in industrial processes it is usually recycled, and as such contains small amounts of the others [5]. The solvent phase leaving the extractor is the extract. the liquid phase left from the feed after being contacted by the extraction solvent is termed raffinate. A schematic extraction process is illustrated in Fig. 2-2.

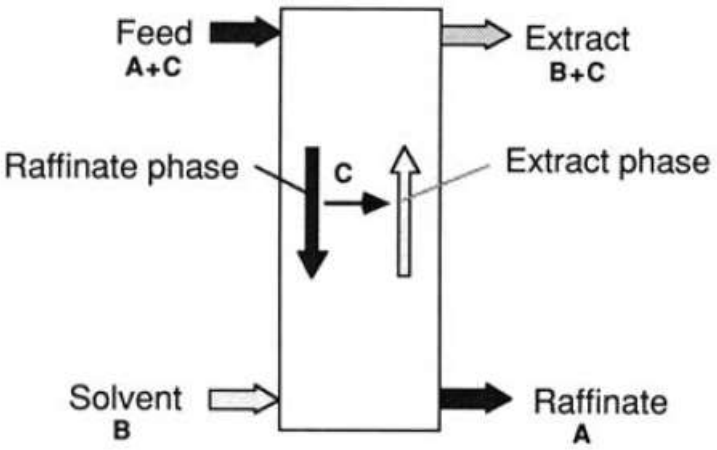

Fig. 2-2 Simplified flow diagram for an extraction column

Extraction takes place inside an equipment called an extractor or an extraction column. It typically contains several stages (plates) in which feed and solvent interact. The number of stages necessary to obtain the desired purity can be estimated based on equilibrium data, in a manner similar to that of distillation columns.

Solvent selection should be based on several considerations [2].

- Selectivity: the relative separation, or selectivity, of a solvent is the ratio of two components in the extraction-solvent phase divided by the ratio of the same components in the feed-solvent phase. It is analogous to relative volatility in distillation.

$$\alpha = \frac{(y_i/x_i)}{(y_j/x_j)}$$

α: the selectivity of the extraction.

y_i: the concentration of component y in the extract.

x_i: the concentration of component x in the raffinate.

y_j: the concentration of component y in the solvent.

x_i: the concentration of component x in the feed.

- Recoverability: The extraction solvent must usually be recovered from the extract stream and also from the raffinate stream in an extraction process.
- Toxicity. Low toxicity from solvent-vapor inhalation or skin contact is preferred because of potential exposure during repair of equipment or while connections are being broken after a solvent transfer. Often solvent toxicity is low if water solubility is high.

2.2 Interfacial properties

The characteristics of the interface between two fluids have been debated by a number of scientists and are still misunderstood.

Van der Waals [3] published one of the first studies on the subject in 1873. In it, he imagined the interface as a finite region, in which physical properties vary continuously from one liquid to another.

In 1892, Lord Rayleigh [4] came to the same conclusion when he measured the light reflection on vapour-liquid interfaces. Based on this model, Cahn and Hilliard [5] developed the Density Gradient Theory (DGT) in 1958.

On the other hand, some authors [9], postulate an interface of zero thickness, meaning all physical quantities are discontinuous across the surface.

2.2.1 Interfacial tension

When two liquids are in contact with each other, the molecules at the surface of separation experience imbalanced forces of attraction. This is what gives way to the interfacial tension between them, which is defined as the force in the plane of the surface per unit length.

This applies to both the interface between two immiscible liquids, as well as the interface between liquid and vapor, in which case it is usually referred to as surface tension.

Surface tension decreases with temperature, and becomes zero at the critical point [7]

Interfacial tension is an important factor in the phenomenon of capillarity and droplet formation, as well as in mass transfer between the phases.

2.2.1.1 Empirical correlations

The interfacial tension between to liquids can be estimated if the surface tensions of each liquid are known [7].

Antonoff's rule predicts that the interfacial tension (γ_{AB}) between two liquids A and B will be equal to the difference between the respective surface tensions (i.e., γ_A and γ_B).

$$\gamma_{AB} = |\gamma_A - \gamma_B|$$

This rules gives a quick value for the interfacial tension, which can be expected to be between the surface tensions of both phases. However, it doesn't hold true for many mixtures.

Girifalco and Good [7] incorporated the effects of the free energies of cohesion of the two phases and the free energy of adhesion on interfacial tension, and proposed the following equation.

$$\gamma_{AB} = \gamma_A + \gamma_B - 2\phi\sqrt{\gamma_A \gamma_B}$$

Where ϕ is a constant defined as

$$\phi = -\frac{\Delta G_{AB}^{a}}{\sqrt{\Delta G_B^c \Delta G_A^c}}$$

ΔG_{AB}^{a} is the free energy of adhesion for the interface between the phases A and B, ΔG_A^c is the free energy of cohesion for phase A, and ΔG_B^c is the free energy of cohesion for phase B.

For many liquid-liquid systems, ϕ lies between 0.5 and 1.2 [8].

2.2.1.2 Direct measurements

Interfacial tension measurement apparatus can be loosely clasified in five categories, based on methodology [11].

1. **Direct measurement using a balance**. Interfacial tension tends to drive interfaces to adopt geometries that minimize the interfacial area, and this tendency can be interpreted as a physical force per unit length (i.e., a tension). The excess energy per unit area (E/A) is numerically equal to this force per unit length (F/L), which is numerically equal to the interfacial tension. When a probe is brought into contact with the interface, the liquid tends to climb up its surface due to capillary force, which increases interfacial area. Thus, the probe experiences a restoring force towards the plane of the interface, which is proportional to the interfacial tension.

2. **Measurement of capillary pressure**. Interfacial tension causes the interface to be as small as possible. Thus, interfaces form curvatures which in turn cause a pressure difference, with the highest pressure on the concave side. This increase in pressure can be measured in a number of ways and used to calculate the tension. A correlation between the two is given by the Young-Laplace equation [12]

$$\Delta P = \gamma(\frac{1}{R_1} + \frac{1}{R_2})$$

Where ΔP is the difference is pressure, γ is the interfacial tension, and R_1 and R_2 are the radii of curvature.

3. **Analysis of the balance between capillary and gravity forces**. Based on observation of capillary effects, like capillary rise or drop volume. They are the oldest known methods and have been largely substituted by modern instruments.

4. **Analysis of gravity-distorted drops**. In absence of external forces like gravity, liquid drops tend to form spherical shapes in order to minimize interfacial area. Thus, a drop's shape is the result of the balance between the capillary and gravitational forces. Bashforth-Adams equation [13] relates these parameters and allows for the calculation of the interfacial tension based on shape.

$$\gamma\left(\frac{\sin\theta}{x} + \frac{1}{R_1}\right) = \frac{2\gamma}{b} + \Delta\rho g z$$

Where γ is the interfacial tension; $\Delta\rho$ is the difference in density between the two fluids, R1 is the radius of curvature; x is the radius of rotation of point S around the z axis; f is the angle of R2 vector with the axis of symmetry; b is the radius of curvature at the apex of the curvature; and g is the acceleration due to gravity. The geometry parameters can be seen in Fig. 2-3.

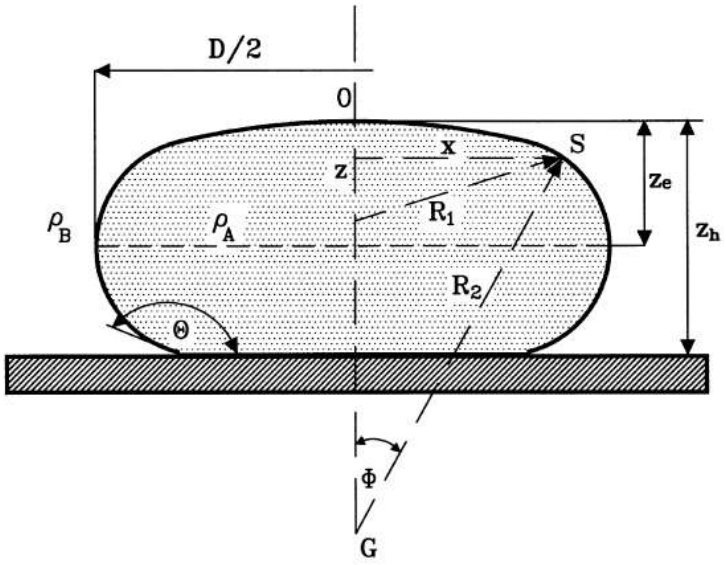

Fig. 2-3 Definition of dimension parameters for the Bashforth-Adams equation

The advantage of shape analysis is that it doesn't require complex instrumentation. The setup usually involves a camera with a low-magnification lens to record the droplet's shape. Interfacial tension can then be calculated from dimensions of the pendant drop, sessile drop, or liquid meniscus. It is also possible to use software for the calculations.

5. **Analysis of drops under centrifugal forces**. Techniques in this group work according to the same principles as those in group 4, but submit the observed drop to centrifugal forces, which allows for the measurement of very low interfacial tensions [11]. Of special interest is the spinning drop technique, which was the method used for this experiment.

In a spinning drop tensometer a drop suspended in a liquid phase is contained in a horizontally mounted capillary. The capillary is then rotated along its longitudinal axis. At low rotational velocities (ω), the fluid drop forms an ellipsoidal shape, but when ω

is sufficiently large, it becomes cylindrical. At the latter condition, the radius *R* of the cylindrical drop is determined by the interfacial tension σ, the density difference $\Delta\rho$ between the drop and the surrounding fluid and the rotational velocity ω of the drop. There are several methods to relate this parameters.

The Vonnegut equation [16] assumes a cylindrical drop with hemispherical ends. This approximation is valid for cases in which the droplet's lenght (L) is at least 4 times larger than its width [15]. In this case, interfacial tension can be expressed as:

$$\sigma = \frac{1}{4}\Delta\rho\omega^2 R^3$$

This is the result of applying an energy balance to the drop, taking into account that the inertial and tension forces are in equilibrium.

The previously discussed Young–Laplace equation rules the relation among curvature, surface energy and pressure difference between two phases. It can be used to describe both spherical and non spherical shapes, and also for the calculation of interfacial tension in a spinning drop tensometer.

Cayias, Schechter and Wade [16] developed a method that takes both the lenght and width of the droplet into account. The resulting equation is more complex and requieres numerical calculations, but is more precise for small droplets.

2.3 Impact of interfacial properties on extraction processes

Mass transfer through an interface depends on several properties and is not fully understood today. Interfacial concentration profiles are not experimentally accessible because of the very small thickness of the interface [1].

Interfacial tension, however, can be experimentally measured and is an important parameter in predictive models.

In extraction, a high interfacial tension promotes rapid coalescence and generally requires high mechanical agitation to produce small droplets. A low interfacial tension allows drop breakup with low agitation intensity but also leads to slow coalescence rates [2].

3 Experimental methods

3.1 Materials

The chemicals used in the experiments are collected in Tab. 3-1. They were used without any further purification.

Tab. 3-1 List of chemicals used in the experiments with their purity and manufacturer.

Chemical	Purity	Manufacturer
Ethanol	99.9%	Merck KGaA
Toluene	99.8%	Lactan
Acetone	99.8%	Lactan
THF	99.8%	Lactan
Purified water	Fully desalinated	-

The equipment used is collected in Tab. 3-2.

Tab. 3-2 List of equipment used during the experiments.

Equipment	Model	Manufacturer
Spinning drop tensometer	Dataphysics SVT 20N	Dataphysics
Gas chromatographer	Agilent GC 6890 N	Agilent
GC column	Agilent J&W DB-624-ui 30m x 0.25mm x 1.4µm	Agilent
Karl-Fischer titrator	Schott TitroLine KF	Schott
Densometer	Anton Paar SVM3000	Anton Paar
Pocket refractometer	Digital Handheld Refractometer PAL-1	Atago

3.2 Analytical methods

Equilibrium data was obtained by preparing mixtures of the water-ethanol-toluene system with varying concentrations, allowing them to reach equilibrium, then analyzing the concentration of each phase.

Concentrations of ethanol, acetone and toluene were determined using gas chromatography (GC). Water content was determined using a Karl-Fischer titrator.

In order to calculate interfacial tensions, the density of each phase, as well as the refractive index of the heavy phase, needed to be determined. This was done using a densometer and a pocket refractometer, respectively. Interfacial tension itself was measured using a spinning drop tensometer.

3.2.1 Gas chromatography

The basic principle of chromatography is that different components travel at different speeds through a stationary phase. This can be used to separate the components of a mixture (preparative chromatography) or to analyze its composition (analytical chromatography). The components are transported throughout the column by a mobile phase.

In gas chromatography, a sample is vaporized and injected onto the head of the chromatographic column. The mobile phase is an inert gas, whereas the stationary phase is a liquid that is adsorbed into the surface of a solid inside the column. The process is schematized in Fig. 3-1.

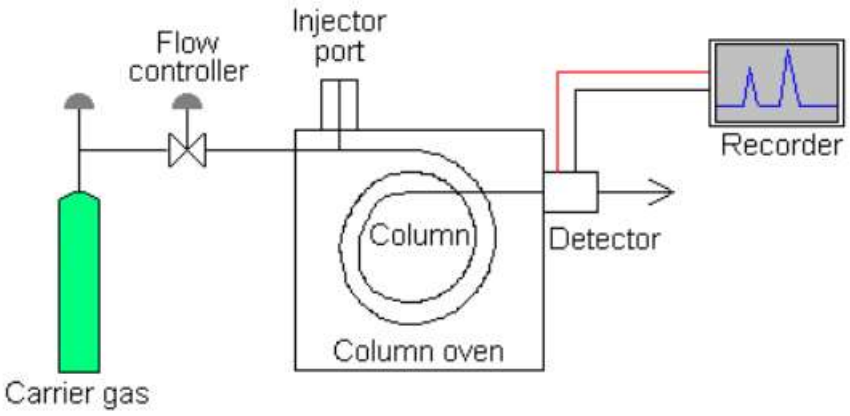

Fig. 3-1 Schematic representation of a GC column [18].

For this experiment the solvent used was tetrahydrofuran (THF) and the carrier gas was hydrogen. The column was an Agilent J&W DB-624-ui, its dimensions 30m x 0.25mm x 1.4µm. The detector was a Flame ionisation detector (FID).

The FID is a general detector for the analysis of organic compounds. In this kind of detector, the effluent from the column is mixed with hydrogen and air, and ignited. Organic compounds burning in the flame produce ions and electrons which can conduct electricity through the flame. A large electrical potential is applied at the burner tip, and a collector electrode is located above the flame. The current resulting from the pyrolysis of any organic compounds is measured. Fig. 3-2 shows a schematic representation of this process.

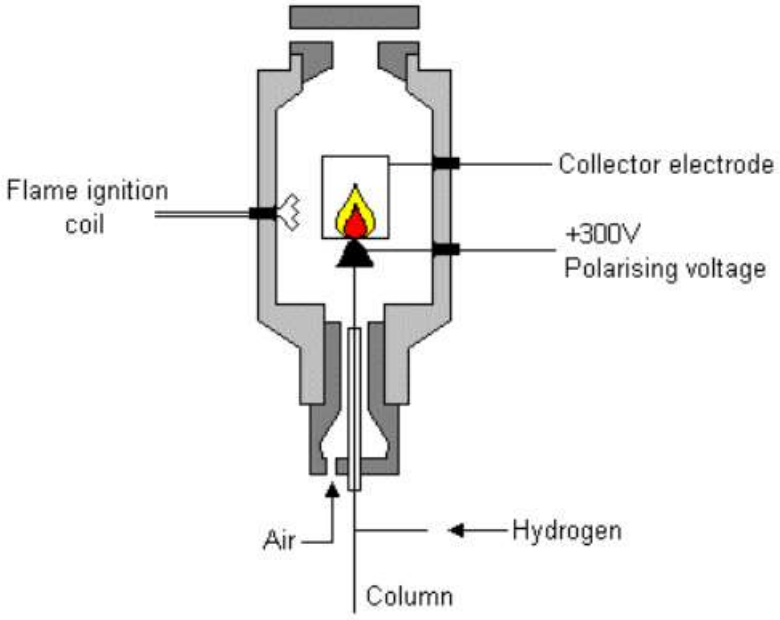

Fig. 3-2 Schematic representation of a FID [18].

The results obtained from gas chromatography are graphics called chromatograms, in which the x axis is time, and the y axis is the intensity of the detector's response. When a component is detected, a peak appears in the graph. The area below this peak is directly proportional to the amount of that compound present in the sample.

Since the components move at different speeds through the stationary phase, they also have different retention times in the column. Therefore, each peak in the chromatogram corresponds to a different compound.

In these experiments it was found that the retention times for the analyzed components was as shown in Tab. 3-3.

Tab. 3-3 Retention times of the sample components in the column

Chemical	Retention time (min)
Ethanol	4.9
Toluene	12.4
Acetone	5.5
THF	solvent

The peak corresponding to ethanol was found to partially separate into two peaks in some samples corresponding to the organic phase. The area below these two peaks was integrated manually and they were interpreted as a single one. The results obtained in this way were consistent with the ones expected, both for retention time and total area.

In order to determine the concentrations based on these areas, a calibration curve is necessary. For a small interval of concentrations, this curve can be assumed to be linear. This means that the relation between peak area and component concentration is a constant.

The GC column only works properly with small concentrations of the measured compounds. Therefore, it was necessary to dilute the samples in THF before measuring them. It was determined that that the concentration of each component should be between 0.2% and 1.5% in mass.

Since the differences in expected concentration between ethanol and toluene were significant, different dilutions were prepared to measure each component. In this way, all concentrations were within the desired range.

The calibration curve was determined by preparing dissolutions of ethanol, acetone, and toluene in THF. Since the mass of each component was known, the concentrations can be plotted against peak area for each component.

The resulting graphs can be seen in figures 3-3, 3-4 and 3-5, along with a corresponding regression curve.

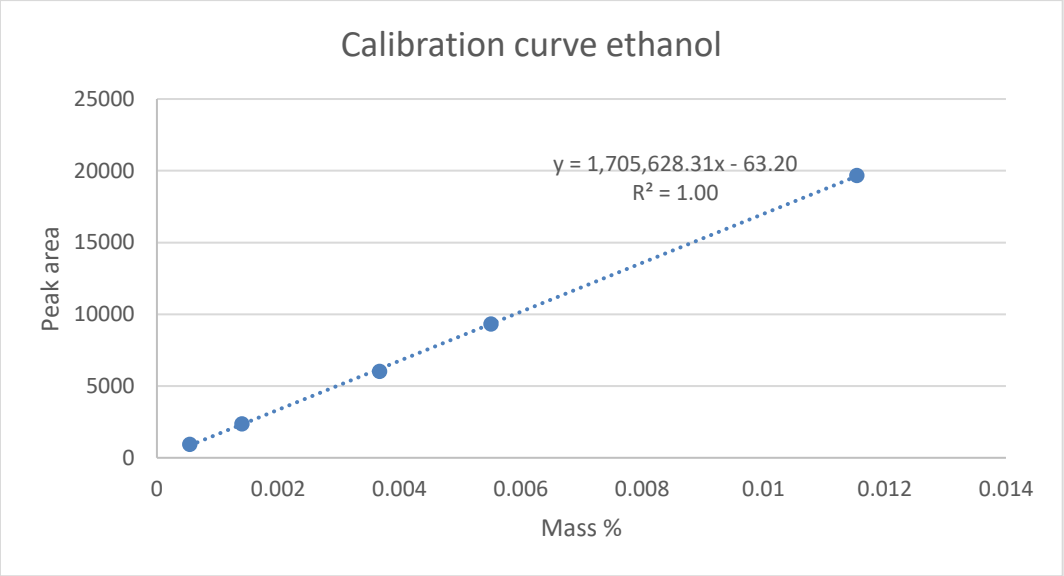

Fig. 3-4 Calibration curve for ethanol

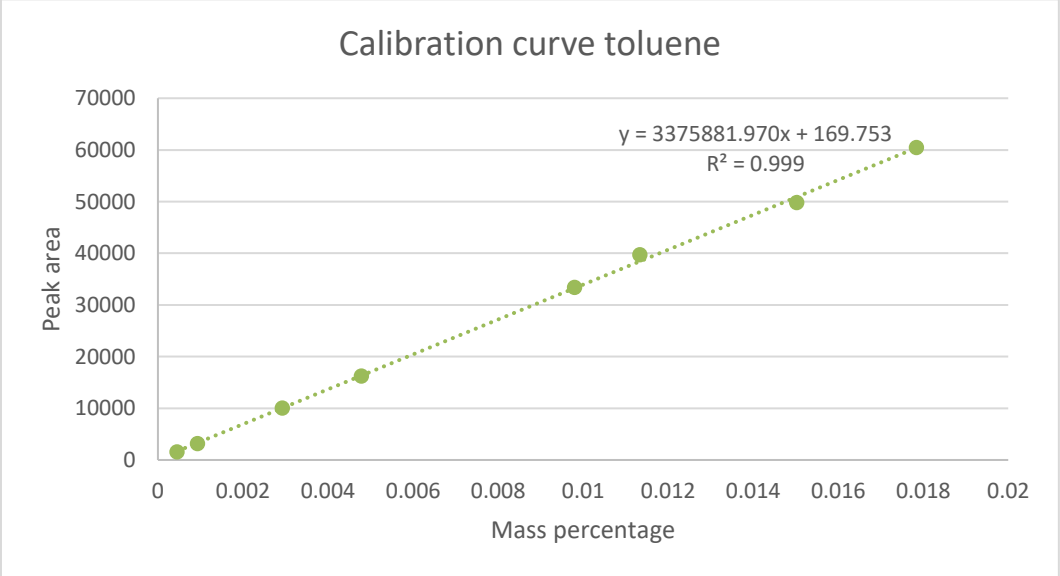

Fig. 3-3 Calibration curve for toluene

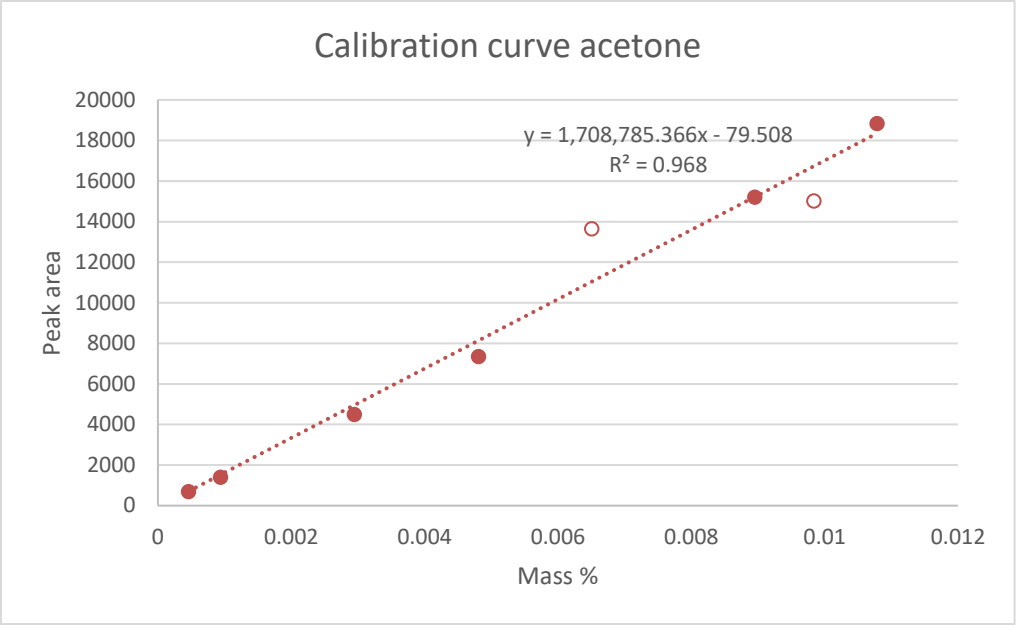

Fig. 3-5 Calibration curve for acetone

As can be deduced from the resulting R^2 values, a linear approximation is valid for the three components. The curve for acetone, however, presents two outliers.

The constants (K) that relate peak area and concentration, in mass %, are the slopes of the regression curves. They are collected in

Tab. 3-4.

Component	K
Ethanol	1,705,628
Toluene	3375882
Acetone	1,708,785

Component	K
Ethanol	1,705,628
Toluene	3375882
Acetone	1,708,785

Tab. 3-4 Calibration constants for each of the components

3.2.2 Karl-Fischer

Karl-Fischer titration is an analytical method in chemistry used to determine traces amount of water in a sample. The volume or mass of reactant used in the titration can be directly correlated with the amount of water introduced with the sample. It was developed by Karl Fischer in 1935 [17]. Modern Karl-Fischer devices automatically pump and measure the reactants and give a result.

The main compartment of the titration cell contains the anode solution plus the analyte. The anode solution consists of an alcohol (ROH), a base (B), SO_2 and I_2. A typical alcohol that may be used is ethanol or diethylene glycol monoethyl ether, and a common base is imidazole.The titration cell also consists of a smaller compartment with a cathode immersed in the anode solution of the main compartment. The two compartments are separated by an ion-permeable membrane.

$$B{\cdot}I_2 + B{\cdot}SO_2 + B + H2O \rightarrow 2BH^{+}I- + BSO_3$$

$$BSO_3 + ROH \rightarrow BH^{+}ROSO_3^{-}$$

The Pt anode generates I2 when current is provided through the electric circuit. The net reaction as shown below is oxidation of SO2 by I2. One mole of I2 is consumed for each mole of H2O. In other words, 2 moles of electrons are consumed per mole of water.

3.2.3 Refractive index

The refractive index or index of refraction of a material is a dimensionless number that describes how light propagates through that medium. It is defined as

$$n = \frac{c}{v}$$

Where c is the speed of light in vacuum and v is the phase velocity of light in the medium. The refractive index determines how much the path of light is bent, or refracted, when entering a material. Therefore, it is necessary to know the refractive

index of the liquid medium in order to correctly interpret images in a spinning drop tensometer.

It can be calculated using Snell's law:

$$n_1 \sin\theta_1 = n_2 \sin\theta_2$$

Where n_1 and n_2 are the refractive indexes of two mediums and θ_1 and θ_2 are the indicent angles of a light ray, as shown in Fig. 3-6.

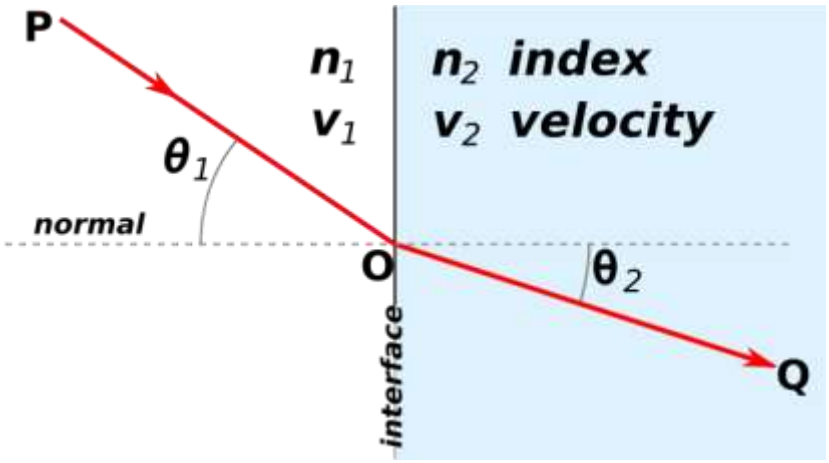

Fig. 3-6 Parameters in Snell's law for light difraction

3.2.4 Spinning drop tensometer

A spinning drop tensometer is a device used to measure interfacial tension between two immiscible phases. It takes advantage of the fact that, when a dropplet is rotated at high speeds, gravitational body forces are negligible. Interfacial tension can then be calculated based on the dropplets form, using different methods (see section 2.2).

The machine used in this experiment was a *Dataphysics SVT 20N.* It included a moving camera and a platform with adjustable slope to position the droplet. Temperature was controlled with a heating unit and kept at 25 °C for the whole process.

The associated software was used to control the device and calculate interfacial tension. In order to take the measurements, the device‘s camera first required calibration. That is, determining the real distance to pixel correlation.

Other necessary data was the density values of both phases and the refractive index of the aqueous phase.

The main challenges encountered during the process were the presence of air bubbles inside the capillar tube, and the separation of the dropplet into smaller ones that were not apt for measurement. In order to obtain a correct measurement, it is necessary that the droplet has an adequate cylindrical form. However, if it is too long its ends might come out of view of the camera. While it is possible to get a measurement this way, it isn't as precise as a measurement using the whole droplet.

An example of this is shown in Fig. 3-7, which depicts a long droplet apt for measurement and two smaller ones. The picture was taken with the device's camera.

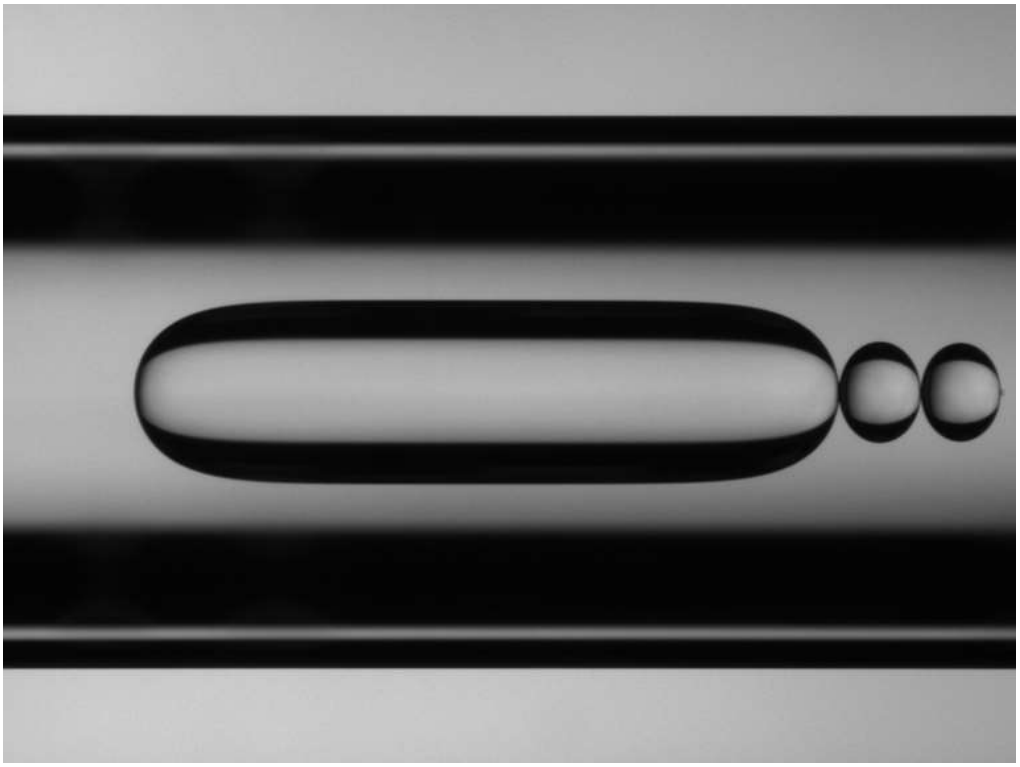

Fig. 3-7 Image of a droplet used in the measurement of interfacial tension of sample 5_2.

A droplet's lenght increases with rotation speed. In order for the measurement to be valid, a minimum lenght is required. Fig. 3-8 illustrates this by graphing interfacial tension as a function of rotation speed for a given sample. For lower rotation speeds the measured values are lower than the correct one and variance is higher. Once a certain speed is reached, the values stabilize.

In general, it was found that the minimum speed required for a proper measurement was 10.000 revolutions per minute. This is consistent with the instruction manual, which states that when the dendity difference between the two phases is low, higher speeds are necessary.

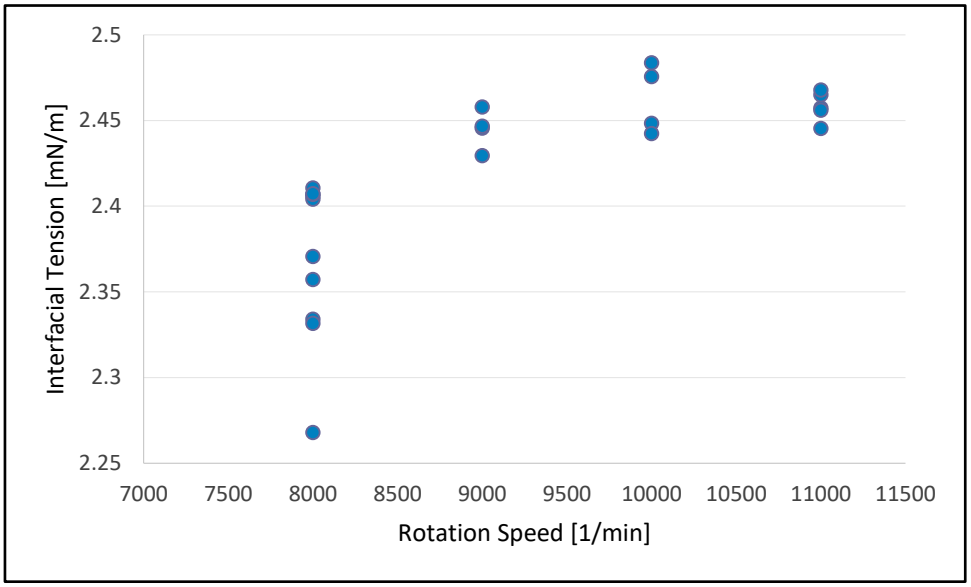

Fig. 3-8 Measured interfacial tension as a function of rotation speed for sample 2_1

3.3 Experiments

3.3.1 Preparation of mixtures

Previous literature shows equilibrium data for the water-ethanol-toluene system at 25 °C [14]. Based on these points, five mixture proportions were arbitrarily selected, such that they'd be located within the two-phase region and there was enough difference in concentration between them that the tie lines obtained would span a wide region of the ternary diagram.

A single mixture of the system water-acetone-toluene was also prepared for the sake of comparison, also based on previous literature [14].

The selected mixtures points are shown in Tab. 3-5

Tab. 3-5 Concentrations of each of the prepared mixtures

Mixture number	Component	Vol %	Mass %
5	Ethanol	20	0.174
	Water	40	0.441
	Toluene	40	0.383
4	Ethanol	25	0.221
	Water	35	0.391
	Toluene	40	0.387
3	Ethanol	30	0.266
	Water	35	0.392
	Toluene	35	0.341
2	Ethanol	35	0.315
	Water	30	0.341
	Toluene	35	0.345
1	Ethanol	40	0.361
	Water	30	0.342
	Toluene	30	0.297
6	Acetone	35	0.33
	Water	25	0.258
	Toluene	40	0.412

A total of 100 ml of each of the six mixtures was prepared, then introduced in flasks suitable for the agitator. The mass of each component was measured using an electronic balance. They were shaken for one hour horizontally, then allowed to rest for four hours vertically for phase separation. Temperature was kept constant at 25 °C using a heat exchanger. Samples from both phases were then taken into smaller vials.

This procedure was repeated 3 times, for a total of 15 equilibrium measurements for the water-ethanol-toluene system, with 5 tie lines measured thrice each.

In between experiments, the flasks were cleaned using acetone and left open to dry at air for one day.

3.3.2 Chromatography

The samples were prepared for chromatography by diluting them in THF. The concentrations were between 1.5% and 0.2% in mass for all components. A calibration curve was determined for this interval by preparing solutions of ethanol, toluene and acetone in THF (see chapter 3.2.1).

3.3.3 Karl-Fischer titrator

Water content was determined using a Karl-Fischer titrator. A volume of approximately 1 ml was retired from the samples using a syringe, and introduced in the machine. Each sample was analyzed three times.

3.3.4 Density measurements

Densities were measured using a Anton Paar SVM3000 viscometer. The unit allowed for temperature control, and all the measurements were taken at 25 °C. Each sample was measured three times.

3.3.5 Refractive index measurement

The refractive index of the heavy (aqueous) phase was measured with an Atago pocket refractometer. The device was calibrated using deionized water. Subsequently, a few droplets were taken from the sample using a syringe, and dropped on top of the measuring lens.

3.3.6 Surface tension measurement

Surface tension measurements were done using a spinning drop tensometer. A capillar tube was filled with the heavy phase, using a syringe. Subsequently, a droplet of the light phase was introduced at the halfway point, using a Hamilton syringe. The capillar

tube was introduced to the spinning drop tensometer and, after ensuring no air bubbles were present, interfacial tension was measured at different rotation frequencies.

After being emptied, the capillar tubes were cleaned by washing with purified water, THF, and acetone. Subsequently, they were dried in a vacuum drier at 120°C for a minimum of two hours.

4 Results and discussion

4.1 Results and discussion of experiments

The samples were numbered from 1 to 6 in each experiment. Samples 1 to 5 are from the water-ethanol-toluene system, and they are in order of decreasing ethanol content, 1 having the highest content and 5 the lowest. Sample 6 is from the water-acetone-toluene system.

The sample corresponding to the organic phase was denoted with an *o* to differentiate it from the aqueous phase.

The experiment was performed three times, and the naming convention was the same each time. Therefore, samples pertaining to the same mixture proportion will be differentiated using a second number from 1 to 3, refering to the experiment in which they were taken.

As an example, sample 2o_3 refers to the sample corresponding to the organic phase of the mixture number 2 in the third experiment.

4.1.1 Chromatography results

Each sample was analyzed twice in the chromatographer. The resulting peak areas from both measurements can be seen in Tab. 4-1 and Tab. 4-2 for ethanol and toluene, respectively, along with the corresponding mass % based on the calibration curves. The absolute difference between the two measurements is also featured.

Acetone measurements are featured in Tab. 4-3. Due to experimental error, sample 6_3 was contaminated, and as such doesn’t appear in the table.

Tab. 4-1 Chromatography results for ethanol

Sample	Peak area 1	Mass % 1	Peak area 2	Mass % 2	Variation
1_1	12965	73.57	11736	66.59	6.97
1_2	8061	42.79	7895	41.91	0.88
1_3	7918	41.99	8170	43.33	1.34
1o_1	7945	5.15	7955	5.16	0.01
1o_2	7283	4.62	7071	4.48	0.13
1o_3	7709	4.87	7775	4.91	0.04
2_1	7727	38.25	7792	38.57	0.32
2_2	6218	38.95	6293	39.42	0.47
2_3	8568	41.77	8759	42.70	0.93
2o_1	7218	4.64	6899	4.44	0.20
2o_2	6769	4.32	6462	4.12	0.20
2o_3	6767	4.36	6830	4.40	0.04
3_1	7233	36.48	6718	33.89	2.60
3_2	7162	35.38	6823	33.71	1.67
3_3	5901	31.13	6411	33.81	2.69
3o_1	5073	3.38	5148	3.43	0.05
3o_2	5254	3.28	5078	3.17	0.11
3o_3	5052	3.22	5066	3.22	0.01
4_1	8342	28.80	8574	29.60	0.80
4_2	4613	32.68	4512	31.97	0.71
4_3	6013	27.96	5912	27.49	0.47
4o_1	3926	2.62	3973	2.65	0.03
4o_2	3936	2.46	3990	2.49	0.03
4o_3	3769	2.44	4011	2.59	0.16

Sample	Peak area 1	Mass % 1	Peak area 2	Mass % 2	Variation
5_1	4301	23.99	4313	24.06	0.07
5_2	4950	24.24	5022	24.59	0.35
5_3	4618	21.87	4745	22.47	0.60
5o_1	2594	1.65	2552	1.62	0.03
5o_2	2488	1.58	2492	1.59	0.00
5o_3	2554	1.60	2621	1.65	0.04

Tab. 4-2 Chromatography results for toluene

Sample	Peak area 1	Mass % 1	Peak area 2	Mass % 2	Variation
1_1	12439	1.84	12256	1.81	0.03
1_2	11903	1.91	11967	1.92	0.01
1_3	7563	1.15	7602	1.16	0.01
1o_1	43883	104.98	44465	106.38	1.39
1o_2	30095	96.57	30274	97.14	0.57
1o_3	26751	81.70	27092	82.74	1.04
2_1	8403	1.25	8360	1.24	0.01
2_2	8351	0.57	8340	0.57	0.00
2_3	5702	0.91	5704	0.91	0.00
2o_1	32824	96.47	32670	96.02	0.45
2o_2	30964	95.14	30236	92.90	2.24
2o_3	28477	91.74	28784	92.73	0.99

Sample	Peak area 1	Mass % 1	Peak area 2	Mass % 2	Variation
3_1	10600	1.60	10700	1.62	0.02
3_2	3573	0.57	3571	0.57	0.00
3_3	1727	0.25	1673	0.24	0.01
3o_1	34438	98.11	33479	95.38	2.73
3o_2	28448	86.26	28244	85.64	0.62
3o_3	27528	94.84	27684	95.37	0.54
4_1	817	0.12	810	0.12	0.00
4_2	2780	0.40	2847	0.41	0.01
4_3	640	0.10	629	0.09	0.00
4o_1	35649	95.60	35303	94.68	0.93
4o_2	32733	113.34	32641	113.02	0.32
4o_3	38037	119.34	38583	121.06	1.71
5_1	1674	0.25	1788	0.27	0.02
5_2	1010	0.15	981	0.15	0.00
5_3	117	0.02	118	0.02	0.00
5o_1	37228	97.63	38213	100.22	2.58
5o_2	36868	115.68	36718	115.20	0.47
5o_3	31659	99.33	31127	97.66	1.67
6_1	159	0.057	166.	0.06	0.00271
6_2	802	0.252	741	0.23	0.0193
6o_1	29734	74.65	29661	74.46	0.185
6o_2	17709	56.4	17659.500	56.24	0.159

Tab. 4-3 Chromatography results for acetone.

Sample	Peak area 1	Mass % 1	Peak area 2	Mass % 2	Variation
6_1	5269	26.249	5181	25.811	0.438
6_2	6215	28.757	6237	28.857	0.099
6o_1	7599	37.688	7607	37.728	0.040
6o_2	4547	28.607	4623	29.086	0.478

As can be seen, the variation in mass percentage between the two measurements is rather small, lower than 1% in most cases and below 3% in all but one. The ethanol content in sample 1_1 is much higher than in 1_2 and 1_3, and its variance is as well, so it can be assumed to be an incorrect measurement.

Toluene content is much higher in the organic phase than in the aqueous one, as would be expected.

4.1.2 Karl-Fischer results

Each sample was measured three times. The results can be seen in Tab. 4-4 and Tab. 4-5 for the organic and aqueous phases, respectively, along with the average value obtained for each sample and the variance.

Tab. 4-4 Karl-Fischer results for the organic samples, in mass percentage.

Sample	Measur. 1	Measur. 2	Measur. 3	Average	σ^2
1o_1	0.469	0.466	0.456	0.464	9.267E-05
2o_1	0.379	0.38	0.368	0.376	8.867E-05
3o_1	0.292	0.278	0.276	0.282	1.520E-04
4o_1	0.194	0.21	0.19	0.198	2.240E-04
5o_1	0.099	0.101	0.0103	0.047	5.950E-03
1o_2	0.496	0.485	0.482	0.488	1.087E-04
2o_2	0.41	0.395	0.39	0.398	2.167E-04
3o_2	0.28	0.269	0.27	0.273	7.400E-05
4o_2	0.24	0.21	0.224	0.224	7.710E-04
5o_2	0.138	0.117	0.117	0.124	2.940E-04
1o_3	0.449	0.442	0.446	0.446	2.467E-05
2o_3	0.398	0.397	0.389	0.395	4.867E-05
3o_3	0.27	0.26	0.269	0.266	6.067E-05
4o_3	0.206	0.206	0.192	0.201	1.307E-04
5o_3	0.125	0.122	0.101	0.115	3.450E-04
6o_1	1.299	1.29	1.316	1.302	3.487E-04
60_2	1.299	1.296	1.285	1.293	1.087E-04

Tab. 4-5 Karl-Fischer results for the aqueous samples, in mass percentage.

Sample	Measur. 1	Measur. 2	Measur. 3	Average	σ^2
1_1	52.206	50.86	53.132	52.058	2.610
2_1	59.849	58.99	55.356	58.032	11.377
3_1	66.827	65.166	65.022	65.667	2.013
4_1	70.805	69.448	72.018	70.749	3.306
5_1	78.826	75.651		77.222	5.040
6_1	78.704	76.841	79.58	78.367	3.913
1_2	52.375	51.822	51.111	51.767	0.803
2_2	57.716	56.233	56.838	56.926	1.112
3_2	64.17	64.771	62.526	63.815	2.701
4_2	69.715	70.418	72.726	70.941	4.962
5_2	80.907	77.148	79.414	79.141	7.165
6_2	79.291	77.48	77.843	78.201	1.836
1_3	56.452	54.269	54.321	55.005	3.103
2_3	57.845	54.38	57.205	56.456	6.799
3_3	65.437	63.707	66.496	65.203	3.964
4_3	72.685	70.865	69.959	71.161	3.855
5_3	79.341	80.059	80.863	80.085	1.159

As can be seen, the values are consistent between measurements and deviation is small.

4.1.3 Tie lines

The concentrations used for the calculation of the tie lines are the averages of the obtained values for each measurement.

In the case of the aqueous phase, since the Karl-Fischer method gives less reliable results for high water concentrations, the results obtained from chromatography were deemed more reliable. Thus, water percentage was calculated from the percentages of toluene and ethanol or acetone.

For the organic phase, the Karl-Fischer results were used. In either case, the results obtained from both methods were consistent.

The 15 tie lines were designated in a manner similar to that of the samples. The equilibrium data can be seen in Tab. 4-6 for the water-ethanol-toluene system, and in Tab. 4-7 for the water-acetone-toluene system.

Tab. 4-6 Equilibrium data for the water-ethanol-toluene system at 25 °C, in mass percentage.

	Aqueous phase			Organic phase		
Tie line	Water %	Toluene %	Ethanol %	Water %	Toluene %	Ethanol %
1_1	28.099	1.823	70.078	0.464	94.384	5.153
1_2	55.736	1.912	42.352	0.488	94.963	4.549
1_3	56.189	1.153	42.658	0.446	94.663	4.891
2_1	60.342	1.247	38.411	0.376	95.087	4.537
2_2	60.250	0.567	39.183	0.398	95.381	4.220
2_3	56.858	0.908	42.234	0.395	95.225	4.381
3_1	63.207	1.608	35.185	0.282	96.317	3.401
3_2	64.890	0.568	34.543	0.273	96.499	3.228
3_3	67.287	0.242	32.471	0.266	96.514	3.220
4_1	70.679	0.121	29.200	0.198	97.165	2.638
4_2	67.267	0.410	32.323	0.219	97.307	2.474
4_3	72.180	0.095	27.725	0.201	97.282	2.517
5_1	75.717	0.259	24.024	0.056	98.309	1.635
5_2	75.434	0.149	24.417	0.124	98.293	1.584
5_3	77.812	0.019	22.169	0.116	98.259	1.625

Tab. 4-7 Equilibrium data for the water-acetone-toluene system at 25 °C, in mass percentage

	Aqueous phase			Organic phase		
Tie line	Water %	Toluene %	Acetone %	Water %	Toluene %	Acetone %
6_1	73.912	0.058	26.030	1.302	60.990	37.708
6_2	70.951	0.242	28.807	1.293	69.860	28.847

The corresponding tie lines are represented graphically in Fig. 4-1, along with the mixing points. The tie lines derived in each of the three experiments can be seen separately in Fig. 4-3, Fig. 4-2 and Fig. 4-4.

Since the measurement of sample 1_1 was deemed incorrect (see secion 4.1.1), its corresponding tie line wasn't included.

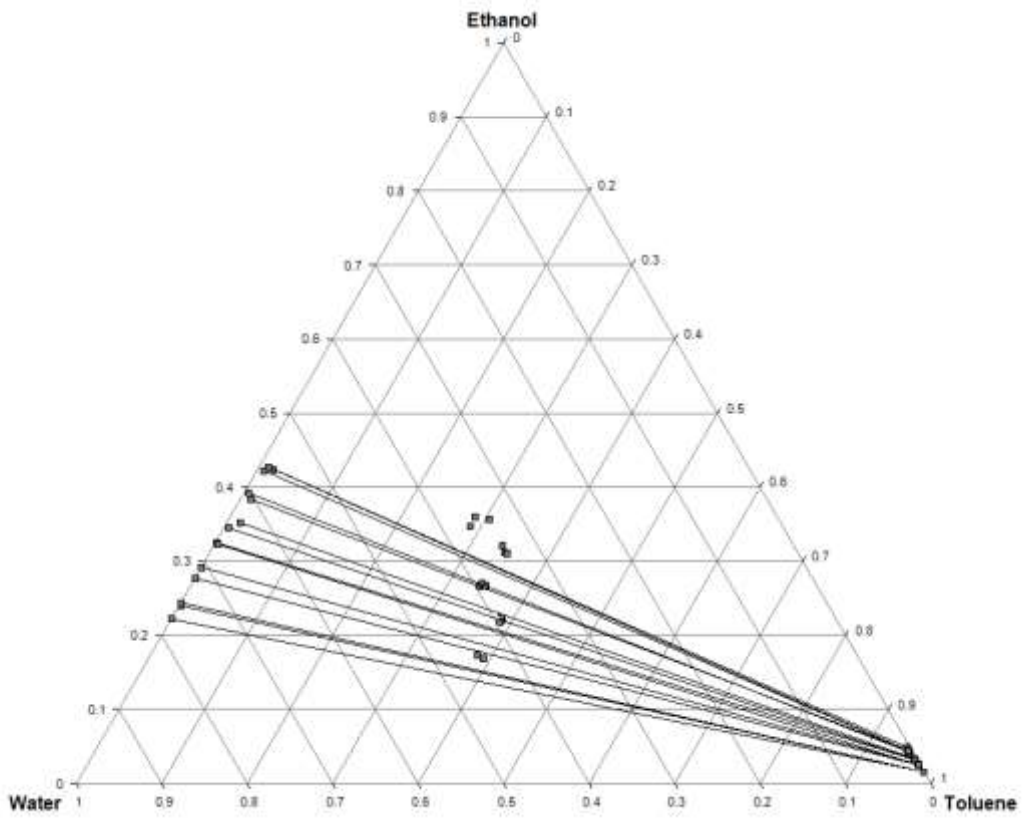

Fig. 4-1 Equilibrium data for the water-ethanol-toluene system at 25 °C. Mixing points for all represented tie lines.

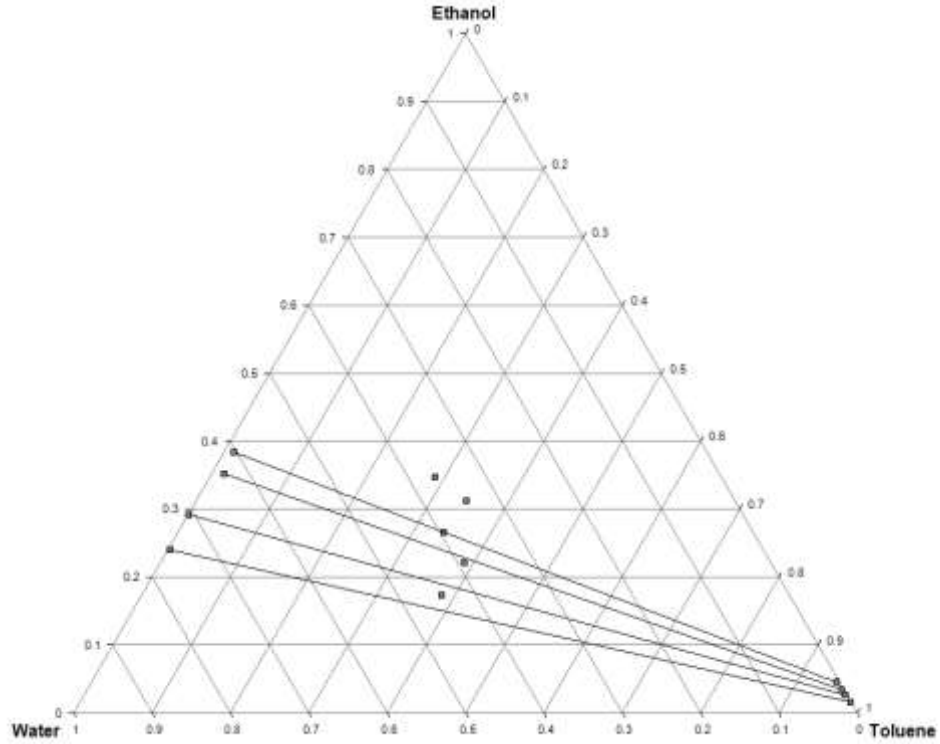

Fig. 4-3 Equilibrium data for the water-ethanol-toluene system obtained in the first iteration of the experiment. Mixing points for all represented tie lines.

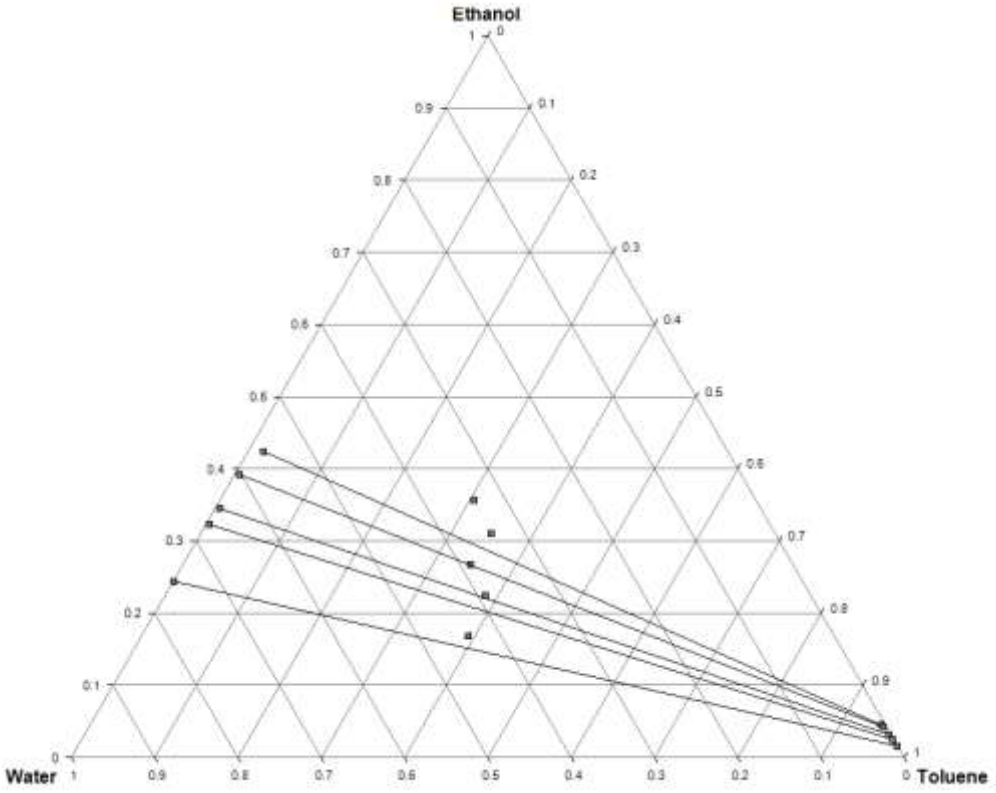

Fig. 4-2 Equilibrium data for the water-ethanol-toluene system obtained in the second iteration of the experiment. Mixing points for all represented tie lines.

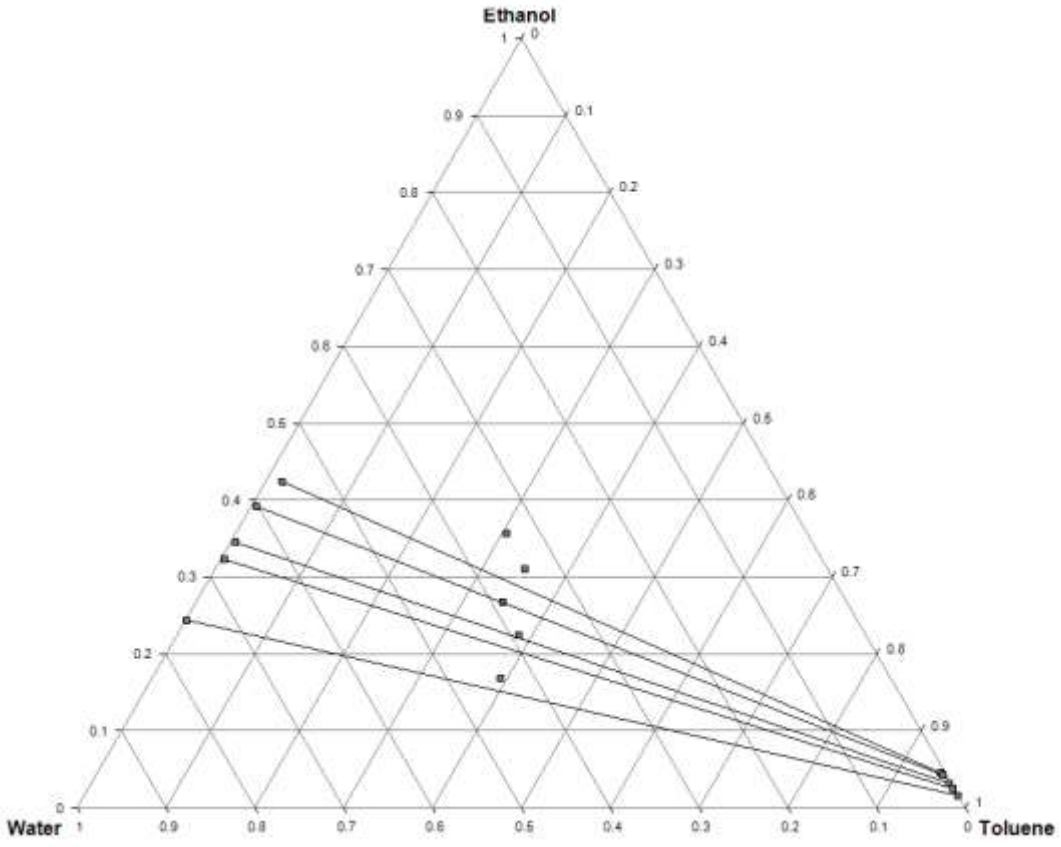

Fig. 4-4 Equilibrium data for the water-ethanol-toluene system obtained in the third iteration of the experiment. Mixing points for all represented tie lines.

Based on these diagrams, there is an obvious offset between the mixing points and their corresponding tie lines. The expected result would be for the slopes to be higher so that the lines crossed the mixing points. This would better fit previous literature [17].

The two tie lines for the water-acetone-toluene system can be seen in Fig. 4-5, along with expected tie lines based on previous literature [22].

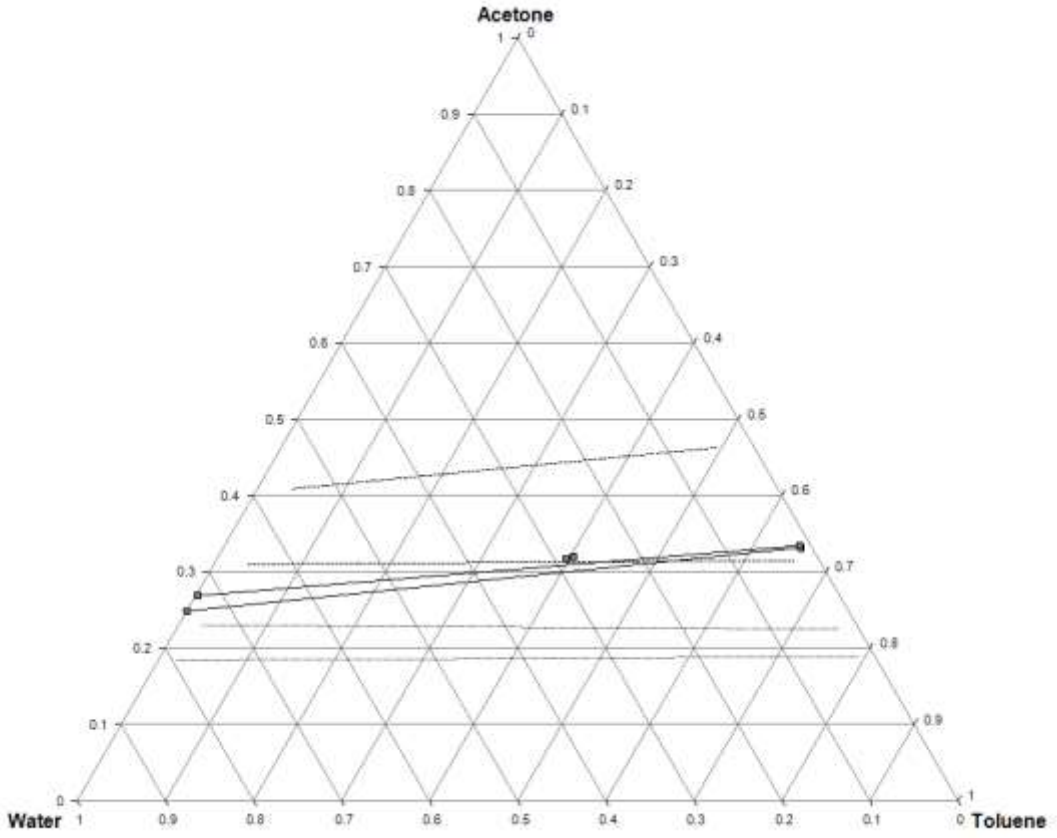

Fig. 4-5 Equilibrium data for the water-acetone-toluene system at 25 °C. Includes expected tie lines based on previous literature (discontinuous lines) [22] and mixing points for all represented tie lines.

Again there is an offset between the tie lines and the mixing points. The slopes of the obtained tie lines don't match the expected slopes.

The inadequacy of the measured data could be caused by experimental inaccuracies. Section 4.2 discussed possible causes of error.

4.1.4 Density measurements

Each sample's density was measured three times. The averaged value of the measured densities can be seen in Tab. 4-8. Also included is the variance for each measurement.

Density values decrease with ethanol content in the aqueous phase. This is to be expected, since ethanol has a lower density than water.

The variance is close to zero in all cases.

Tab. 4-8 Average density values for each sample at 25 °C, in kg/m^3

	Aqueous phase		Organic phase	
Sample	Density	σ^2	Density	σ^2
1.1	0.908	4.667E-08	0.857	2.000E-08
1.2	0.908	5.000E-09	0.857	6.667E-09
1.3	0.911	2.000E-08	0.858	2.667E-08
2.1	0.917	1.800E-07	0.858	6.667E-09
2.2	0.917	5.267E-07	0.858	6.667E-09
2.3	0.917	6.000E-08	0.858	6.667E-09
3.1	0.933	1.667E-07	0.859	8.667E-08
3.2	0.932	5.067E-07	0.859	1.400E-07
3.3	0.933	1.267E-07	0.859	2.867E-07
4.1	0.945	0.000E+00	0.859	4.667E-08
4.2	0.944	2.000E-08	0.859	2.000E-08
4.3	0.944	3.267E-07	0.859	6.000E-08
5.1	0.956	2.000E-08	0.860	2.667E-08
5.2	0.957	6.667E-09	0.861	8.667E-08
5.3	0.958	6.000E-08	0.861	3.698E-32
6.1	0.962	6.667E-09	0.838	4.667E-08
6.2	0.958	2.000E-08	0.838	4.667E-08

4.1.5 Refractive index measurements

For determination of interfacial tensions by the spinning drop method the refractive index of the heavy phase has to be known. Thus, refractive indices of the aqueous samples were measured as described in chapter 3.2.3. The measured refractive indexes are collected in Tab. 4-9 .

Tab. 4-9 Refractive indexes for the measured samples at ambient temperature

Sample	Refractive index
1.1	1.359
1.2	1.348
1.3	1.361
2.1	1.357
2.2	1.363
2.3	1.358
3.1	1.347
3.2	1.358
3.3	1.356
4.1	1.339
4.2	1.350
4.3	1.354
5.1	1.332
5.2	1.350
5.3	1.351
6.1	1.350
6.2	1.352

4.1.6 Interfacial tension measurements

The averaged interfacial tension values for each sample are collected in Tab. 4-10. The measurements were taken at different rotation speeds. The values for which the speed was deemed too low were ignored (see section 3.2). A droplet of toluene in water was also measured to serve as a reference.

Tab. 4-10 Interfacial tension values of the samples and ethanol content at 25 °C.

Sample	Interfacial tension (mN/m)	Ethanol mass %
1_1	1.581	0.565
1_2	2.460	0.441
1_3	2.191	0.432
2_1	1.876	0.393
2_2	2.719	0.405
2_3	2.506	0.424
3_1	4.514	0.343
3_2	4.217	0.349
3_3	3.727	0.332
4_1	5.654	0.292
4_2	4.965	0.312
4_3	4.794	0.280
5_1	8.137	0.237
5_2	8.315	0.235
5_3	7.938	0.217
Toluene-Water	26.959	0

Based on this results, there is an obvious correlation between ethanol content and interfacial tension. Fig. 4-6 shows this correlation, along with literature data obtained via the capillary rise method [23].

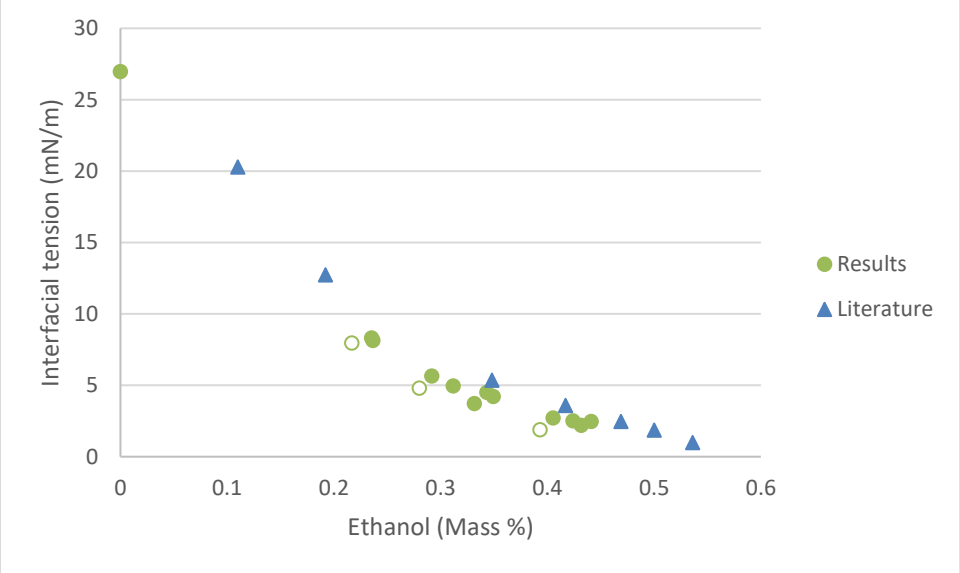

Fig. 4-6 Measured interfacial tension as a function of ethanol concentration, along with literature data on the same system [23].

Samples 2_1, 4_3 and 5_3, marked in white in Fig. 4-7, appear to have a lower interfacial tension than in literature. Sample 1_1, while in line with the expected result, was deemed to be incorrectly measured due to its apparent ethanol content (see section 4.1.1).

4.2 Error discussion

Posterior analysis of the experimental methods used shows several weaknesses in the work that could explain the inadequacy of the data.

The mixtures were prepared in a separate flask, then moved to one suitable for the mixer. It is possible that this caused the components proportion to change due to residual matter in the flask, which may not have had the same composition as the overall mixture.

Both phases were extracted from the flask using a valve at the bottom. This could have caused the light phase samples to be contaminated with residual heavy phase.

The samples were kept in a fridge between measurements. The low temperature could cause the miscibility of the components to change, leading to phase separation. While they were kept outside before a measurement so they would reach room temperature,

no temperature measurement was taken. It is possible that the samples were still below the desired 25 °C at the time they were extracted from the vials.

Posterior work accounted for these potential sources of error. The mixtures were prepared directly in the vials where the measurements took place. Samples were extracted using a syringe. The sample vials were left in the temperature bath for a total of 29 hours and samples were withdrawn after 23 and 29 hours to ensure that the equilibrium had been reached, and were kept at room temperature. The results obtained in this way fit previous literature much better. These results can be seen in Fig. 4-8. In this case the tie lines fit the mixing points, and their slopes are consistent with previous research.

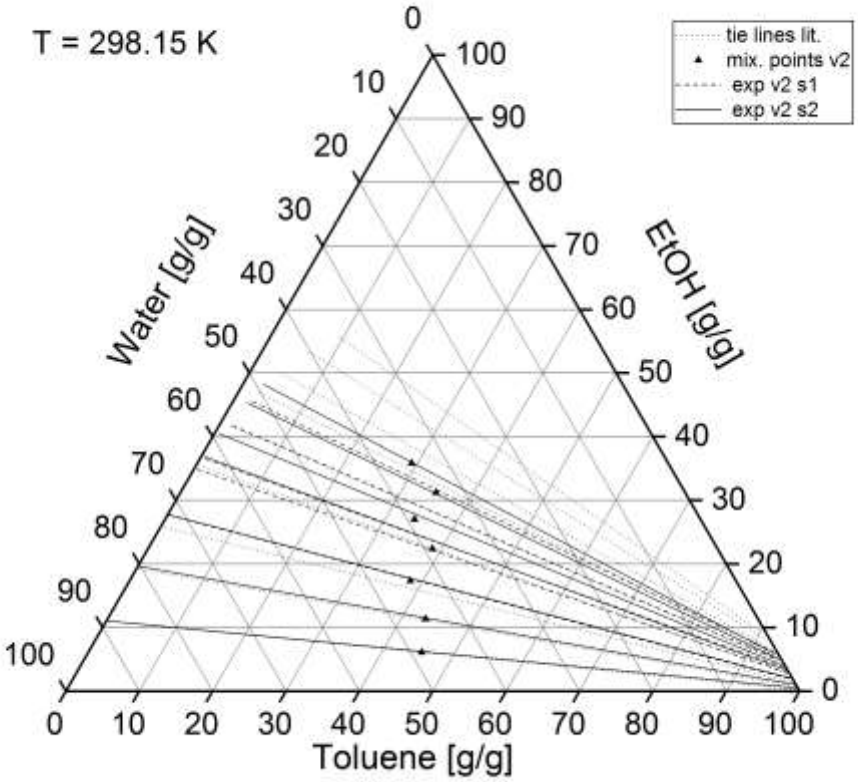

Fig. 4-8 Equilibrium data for the water-ethanol-toluene system at 25 °C. Obtained from a posterior experiment.

5 Summary and outlook

Equilibrium data for the water-ethanol-toluene system was experimentally determined. Five equilibrium points were analyzed at 25 °C, and each point was measured three times. Concentrations were determined using gas chromatography for toluene and ethanol, and a Karl-Fischer titrator for water.

The tie lines obtained were found to be consistent, but inadequate, and didn't fit previous literature data. There was a significant offset between the obtained tie lines and the mixing points, and the tie lines' slopes were lower than expected based on previous experiments. This was almost certainly due to experimental inaccuracies, which were accounted for in posterior measurements. Namely, the samples were kept in a fridge between measurements and the mixtures weren't prepared directly in the vials used for measurement, which could've changed their composition. Subsequent work yielded results that much better fit literature data.

Interfacial tension, density and refractive index were also measured for the same points. The equipment used was a spinning drop tensometer. Interfacial tension was found to decrease with ethanol content. Measured data was consistent with previous literature data.

The obtained data will be the basis for posterior work on interfacial mass transfer modelling. Future experiments related to this ternary system include observation of mass transfer rate in a Nitsch cell, as well as viscosity measurements.

6 Appendix

6.1 References

[1] Feindt, P. D. K. Sattler and D. H. Jacob, Thermal Separation Processes: Principles and Design, VCH Verlagsgesellschaft mbH, 2007.

[2] K. F. Kruber, M. Krapoth and T. Zeiner, "Interfacial mass transfer in ternary liquid-liquid systems," *Fluid Phase Equilibria*, vol. 440, pp. 54-63, 2017.

[3] T. Grunert, "Theoretical and Experimental Studies on Interfacial Properties of Ternary Liquid Mixtures," 18 August 2014. [Online]. Available: http://dx.doi.org/10.14279/depositonce-4146.

[4] R. H. Perry, Perry's Chemical Engineer's Handbook - Seventh Edition, The McGrawHill Companies, 1997.

[5] E. Müller, R. Berger, E. Blass, D. Sluyts and A. Pfennig, "Liquid–Liquid Extraction," in *Ullmann's Encyclopedia of Industrial Chemistry*, 2008.

[6] J. D. Van der Waals, *Over de Continuiteit van den Gas en Vloiestoftoestand (On the Continuity of the Gas and Liquid State).*, Leiden University, 1873.

[7] L. Rayleigh, "On Reflexion from Liquid Surfaces in the Neighbourhood of the Polarizing Angle," *Philos. Magn*, no. 33, pp. 1-18, 1892.

[8] J. W. Cahn and J. E. Hilliard, "Free Energy of a Nonuniform System. I. Interfacial Free Energy.," *The Journal of Chemical Physics*, no. 28, pp. 258-267, 1958.

[9] D. Anderson, G. McFadden and A. Wheeler, "Diffuse-interface methods in fluid mechanics," *Ann. Rev. Fluid Mech.*, vol. 30, pp. 139-165, 1998.

[10] J. J. Jasper, "The Surface Tension of Pure Liquid Compounds," *Journal of Physical and Chemical Reference Data*, vol. 1, p. 841, 1972.

[11] D. P. Ghosh, *Interfacial Tension*, IIT Guwahati.

[12] L. A. Girifalco and R. J. Good, "A Theory for the Estimation of Surface and Interfacial Energies. I. Derivation and Application to Interfacial Tension," *J. Phys. Chem*, vol. 61, p. 904–909, 1957.

[13] J. &. F. Drelich and C. Ch & White, "Measurement of interfacial tension in Fluid-Fluid Systems," in *Encyclopedia of Surface and Colloid Science*, 2002, pp. 3152-3166.

[14] T. Young, "Miscellaneous Works," vol. 1, J. Murray, 1855, p. 418.

[15] F. Bashforth and J. Adams, An Attempt to test the Theory of Capillary Action, London: Cambridge University Press, 1883.

[16] A. Couper, R. Newton and C. Nunn, "A simple derivation of Vonnegut's equation for the determination of interfacial tension by the spinning drop technique," *Colloid & Polymer Science*, vol. 261, pp. 371-372, 1983.

[17] J. Viades-Trejo and J. Gracia-Fadrique, "Spinning drop method; from Young–Laplace to Vonnegut," *Colloids and Surfaces*, 2006.

[18] J. L. CAYIAS, R. S. SCHECHTER and W. H. WADE, "The Measurement of Low Interfacial Tension via the Spinning Drop Technique," in *ACS Symposium Series*, vol. 8, AMERICAN CHEMICAL SOCIETY, 1975, p. 234–247.

[19] K. Fischer, "Neues Verfahren zur maßanalytischen Bestimmung des Wassergehaltes von Flüssigkeiten und festen Körpern," *Angew. Chem.*, vol. 48, p. 394–396, 1935.

[20] J. Sorensen and W. Art, in *Liquid - Liquid Equilibrium Data Collection*, pp. 1979-1980.

[21] J. H. WALTON and J. D. JENKINS, "A study of the ternary system, toluene-acetone-water," 1923.

[22] T. J. Afolabi and T. I. Edewor, "Liquid-Liquid Equilibrium Data for Butan-2-ol - Ethanol - Water, Pentan-1-ol - Ethanol - Water and Toluene - Acetone - Water Systems," *International Journal of Chemical and Molecular Engineering,* vol. 5, no. 12, 2011.

[23] E. Sada, S. Kite and M. Yamashita, "Interfacial Tensions of Two-Phase Ternary Systems," *Journal of Chemical and Engineering Data,* vol. 20, no. 4, 1975.

[24] Heardhome, 2018. [Online]. Available: Heardhome.com.

[25] S. H. University, "Gas chromatography," [Online]. Available: https://teaching.shu.ac.uk/hwb/chemistry/tutorials/chrom/gaschrm.htm. [Accessed 27 6 2018].

6.2 List of Figures

6.3 List of Tables